

# Phase Behavior of Medium and High Internal Phase Water-in-Oil Emulsions Stabilized Solely by Hydrophobized Bacterial Cellulose Nanofibrils

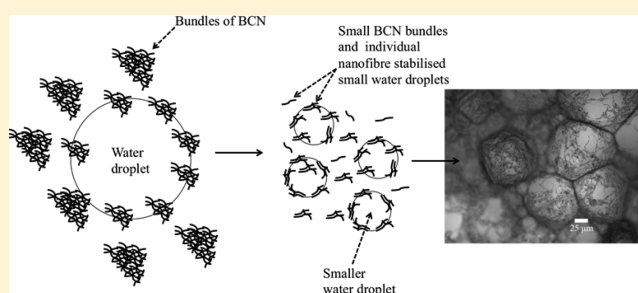
Koon-Yang Lee,<sup>†,‡,⊥</sup> Jonny J. Blaker,<sup>‡</sup> Ryo Murakami,<sup>||</sup> Jerry Y. Y. Heng,<sup>§</sup> and Alexander Bismarck<sup>\*,†,‡</sup>

<sup>†</sup>Polymer and Composite Engineering (PaCE) Group, Institute of Materials Chemistry and Research, Faculty of Chemistry, University of Vienna, Währinger Strasse 42, A-1090 Vienna, Austria

<sup>‡</sup>Polymer and Composite Engineering (PaCE) Group and <sup>§</sup>Surfaces and Particle Engineering Laboratory (SPEL), Department of Chemical Engineering, Imperial College London, South Kensington Campus, London SW7 2AZ, United Kingdom

<sup>||</sup>Department of Chemistry of Functional Molecules, Konan University, 8-9-1 Okamoto, Kobe 658-8501, Japan

**ABSTRACT:** Water-in-oil emulsions stabilized solely by bacterial cellulose nanofibers (BCNs), which were hydrophobized by esterification with organic acids of various chain lengths (acetic acid, C<sub>2</sub>; hexanoic acid, C<sub>6</sub>; dodecanoic acid, C<sub>12</sub>), were produced and characterized. When using freeze-dried C<sub>6</sub>-BCN and C<sub>12</sub>-BCN, only a maximum water volume fraction ( $\phi_w$ ) of 60% could be stabilized, while no emulsion was obtained for C<sub>2</sub>-BCN. However, the maximum  $\phi_w$  increased to 71%, 81%, and 77% for C<sub>2</sub>-BCN, C<sub>6</sub>-BCN, and C<sub>12</sub>-BCN, respectively, 150 h after the initial emulsification, thereby creating high internal phase water-in-toluene emulsions. The observed time-dependent behavior of these emulsions is consistent with the disentanglement and dispersion of freeze-dried modified BCN bundles into individual nanofibers with time. These emulsions exhibited catastrophic phase separation when  $\phi_w$  was increased, as opposed to catastrophic phase inversion observed for other Pickering emulsions.



## 1. INTRODUCTION

The pioneering work of Ramsden<sup>1</sup> and Pickering<sup>2</sup> in the early 20th century showed that colloidal particles can adsorb at fluid–fluid interfaces to form stable emulsions. These particle-stabilized emulsions are now commonly known as Pickering or Ramsden emulsions (the phrase “Pickering emulsions” is more commonly used). The condition for the formation of either an oil-in-water (o/w) or a water-in-oil (w/o) emulsion was formulated by Finkle et al.<sup>3</sup> If the particles possess intermediate wettability, they tend to adsorb at interfaces, and if sufficient particles are available to occupy the interface, the particles will cause the interface to bend toward the more poorly wetting liquid. A relationship between this bending of the fluid–fluid interface and the three-phase contact angle was later put forward by Scarlett et al.<sup>4</sup> If the three-phase contact angle is slightly less than 90°, the particles will cause the fluid–fluid interface to bend toward the oil phase, leading to the formation of o/w emulsions. Conversely, if the three-phase contact angle is slightly higher than 90°, the particles will cause the fluid–fluid interface to bend toward the water phase, leading to the formation of w/o emulsions.

Numerous authors have derived and rederived the condition for attaining the maximum stability of particle-stabilized emulsions mathematically.<sup>5–7</sup> This mathematical relationship relates the energy required to remove a particle from the fluid–fluid interface ( $\Delta E$ ) to the three-phase contact angle ( $\theta$ ):

$$\Delta E = \pi r^2 \gamma (1 \pm \cos \theta)^2 \quad (1)$$

where  $r$  and  $\gamma$  represent the radius of the particle and the fluid–fluid interfacial tension, respectively. The positive sign refers to the removal of a particle into the oil phase, while the negative sign refers to the removal of a particle into the water phase. The magnitude of  $\Delta E$  is usually orders of magnitude larger than the thermal energy,  $kT$ , for particles with intermediate wettability. In addition to the large energy required to remove particles from the fluid–fluid interface, particle-stabilized emulsions offer several advantages over conventional surfactant-stabilized emulsions: (i) improved emulsion stability toward droplet coalescence and (ii) reduced rate of creaming/sedimentation due to an increase in viscosity of the emulsions as a result of aggregation of excess particles in the continuous phase.<sup>8,9</sup> The stability of particle-stabilized emulsions depends on the particle concentration and particle–particle interaction. At high particle concentrations, the particles adsorbed irreversibly at the interface will act as a mechanical barrier against droplet coalescence.<sup>10</sup> In addition to this, the formation of a three-dimensional particle network in the continuous phase impedes the coalescence of the dispersed droplets.<sup>11</sup> The stabilization mechanism of particle-stabilized emulsions at low particle concentration however differs; here limited coalescence and

Received: May 5, 2013

Published: December 27, 2013

Table 1. Pickering Emulsions Stabilized by Various Types of Cellulose<sup>14–22,24,54–56</sup>

type of cellulose	chemical modification	oil phase	type of emulsion	$\phi^a$ (vol %)
microcrystalline cellulose		heavy mineral oil	o/w	20
		sunflower oil	o/w	20
		vegetable oil	o/w	50
		kerosene	o/w	50
nanofibrillated cellulose <sup>b</sup>	silylation with chlorodimethylisopropylsilane neat <sup>c</sup> modified with octadecylamine <sup>c</sup> modified with poly(styrene-co-maleic anhydride) <sup>c</sup>	toluene	w/o	20–50
		diesel	w/o	10–20
			w/o	10–20
microfibrillated cellulose <sup>b</sup>		vegetable oil	o/w	50
		kerosene	o/w	50
cellulose nanocrystals	hydrolyzed with H <sub>2</sub> SO <sub>4</sub> hydrolyzed with H <sub>2</sub> SO <sub>4</sub> , followed by desulfonation step hydrolyzed with HCl hydrolyzed with HCl, followed by sulfonation step hydrolyzed with HCl	<i>n</i> -hexadecane	o/w	30
			o/w	92
bacterial cellulose	hydrolyzed with H <sub>2</sub> SO <sub>4</sub> , followed by poly(NIPAM) grafting  silylation with chlorodimethylisopropylsilane esterified with acetic acid	heptane	o/w	50
		vegetable oil	o/w	50
		kerosene	o/w	50
		acrylated epoxidized soybean oil	w/o or o/w <sup>d</sup>	30–60
		w/o	60	

<sup>a</sup> $\phi$  denotes the volume fraction of the dispersed phase. <sup>b</sup>The difference between nanofibrillated cellulose and microfibrillated cellulose is the dimension of the fibers. <sup>c</sup>In these formulations, a combination of glycerol monooleate and sorbitan monolaurate was also added into the emulsions along with the cellulose particles to stabilize the emulsions. <sup>d</sup>The type of emulsion depends on the volume fraction of the oil phase used.

bridging of droplets by a monolayer of particles are the dominant stabilization mechanisms.<sup>10,12</sup> Numerous types of colloidal particles have been investigated as potential particles to produce particle-stabilized emulsions. These include silica, clay particles, polymeric particles, such as polystyrene and poly(tetrafluoroethylene),<sup>9</sup> and microgel particles, such as lightly cross-linked poly(vinylpyridine) with silica.<sup>13</sup> However, there are very few studies that investigate renewable particulate emulsifiers. In this context, cellulose is one of the best candidates due to its wide availability and nontoxic nature.

The use of cellulose particles as particulate emulsifiers was first described by Oza and Frank,<sup>14</sup> who used food-grade microcrystalline cellulose to stabilize heavy mineral oil-in-water emulsions. Other types of cellulose have also been used as particulate emulsifiers, which include microfibrillated cellulose,<sup>15</sup> nanofibrillated cellulose,<sup>16–19</sup> cellulose nanocrystals,<sup>20–23</sup> and bacterial cellulose nanofibrils.<sup>15</sup> Table 1 gives a brief summary of the emulsions stabilized by various types of cellulose particles to date, using different types of oil phases and the achieved dispersed volume fractions ( $\phi$ ). It can be seen that the hydrophilic nature of pure cellulose always resulted in the formation of o/w emulsions. To produce w/o emulsions, the cellulose had to be hydrophobized sufficiently to bend the interface toward the water phase. More importantly, Table 1 shows that only low internal phase (ratio) (LIPE) and medium internal phase (ratio) (MIPE) emulsions had been produced. However, during the preparation of this paper, a paper on high internal phase o/w emulsions stabilized by cellulose nanocrystals was published.<sup>23</sup> A previous study by us showed the effect of varying  $\phi_w$  on the stability and behavior of water-in-acrylated epoxidized soybean oil emulsions.<sup>24</sup> It was found that the w/o emulsions undergo catastrophic phase inversion to o/w emulsions when  $\phi_w$  was increased beyond 60 vol %. This implied that we only managed to prepare MIPEs. We are, however, interested to go beyond MIPEs and prepare stable w/

o high internal phase emulsions (HIPEs). Water-in-oil HIPEs have several advantages:<sup>25</sup> (i) high  $\phi_w$  causes the emulsions to gel, which suppresses sedimentation, (ii) a low amount of organic phase is needed, and (iii) when a monomer is used as the oil phase, highly porous polymers can be produced.<sup>26</sup> Therefore, in this work we show that stable w/o HIPEs stabilized by hydrophobized bacterial cellulose nanofibrils (BCNs) can be produced. Contrary to our previous study,<sup>24</sup> we show that these emulsions do not undergo catastrophic phase inversion but a catastrophic phase separation that is reversible.

## 2. MATERIALS AND METHODS

**2.1. Materials.** Toluene (analaR NORMAPUR, purity  $\geq 99.5\%$ ), acetic acid (analaR, purity  $\geq 99\%$ ), methanol (GPR, purity  $\geq 99\%$ ), ethanol (GPR, purity  $\geq 99\%$ ), and pyridine (analaR NORAMPUR, purity  $\geq 99.7\%$ ) were purchased from VWR International Ltd. Dimethyl carbonate (Aldrich Reagent Plus, purity  $\geq 99\%$ ), hexanoic acid (purity  $\geq 99.5\%$ ), dodecanoic acid (purity  $\geq 98\%$ ), and *p*-toluenesulfonyl chloride (purity  $\geq 99\%$ ) were purchased from Sigma-Aldrich. Sodium hydroxide (purum grade, pellets) was purchased from Acros Organics. All the materials were used without further purification. BCN was extracted from commercially available nata de coco (CHAOKOH coconut gel in syrup, Ampol Food Processing Ltd., Nakorn Pathom, Thailand).

**2.2. Extraction and Surface Modification of BCN.** The extraction, purification, and modification of BCN with acetic acid, hexanoic acid, and dodecanoic acid were published in previous work,<sup>27,28</sup> but briefly, the gels from ten 500 g jars of nata de coco were rinsed with deionized water to wash away the sugar syrup. The washed nata de coco gels were blended for 1 min using a laboratory blender (Waring Blender LB20EG, Christison Particle Technologies, Gateshead, U.K.) and then homogenized (Polytron PT 10-35 GT, Kinematica, Lucerne, Switzerland) for 2 min. This blend was then centrifuged at 14000g to remove the excess water. BCN was further purified by redispersing it in 10 L of 0.1 N sodium hydroxide solution. This mixture was heated to 80 °C for 20 min while being stirred to remove any soluble polysaccharides.<sup>29</sup> The purified BCN was then

successively centrifuged and homogenized back to neutral pH using deionized water. The morphology of the purified BCN is shown in Figure 1. These fibers are approximately 50 nm in diameter and several

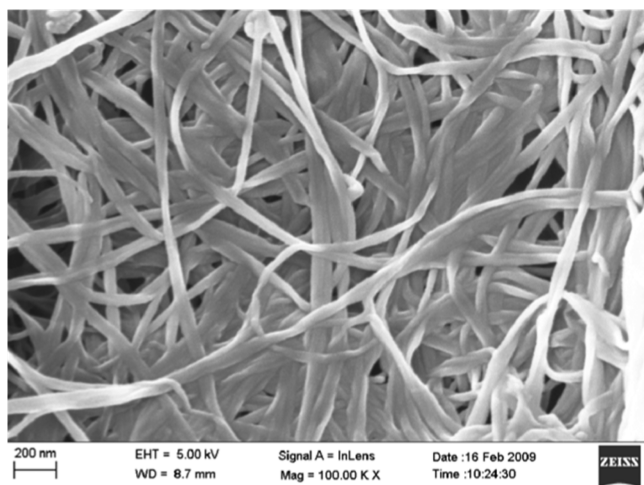


**Figure 1.** Scanning electron micrograph of purified BCN used in this work. Reprinted with permission from ref 28. Copyright 2011 Springer.

micrometers long. However, it should be noted that the length of an individual bacterial cellulose nanofiber is difficult to quantify, as BCN normally exists as a fibrous network.<sup>30</sup>

The surface hydrophobization of BCN starts with solvent exchanging 2 g (dry weight basis) of the purified BCN from water through methanol ( $3 \times 600 \text{ cm}^3$ ) into pyridine ( $2 \times 600 \text{ cm}^3$ ). A solvent exchange step was needed instead of freeze-drying neat BCN and redispersing it in the subsequent reaction medium because we observed severe bulk modification when modifying freeze-dried BCN.<sup>31</sup> The BCN mixture was homogenized at 20000 rpm for at least 1 min at each stage to completely disperse BCN in the solvent. The BCN was retained by centrifugation at 14000g. Another solvent exchange step was performed to adjust the final concentration of BCN in pyridine to  $0.5\% \text{ (g cm}^{-3}\text{)}$ . This BCN–pyridine mixture was poured into a 1 L three-neck round-bottom flask and stirred using a magnetic stirrer. A 92 g portion of *p*-toluenesulfonyl chloride (TsCl) was added into the reaction flask followed by an equimolar amount of organic acid. The reaction was conducted for 2 h at  $50 \text{ }^\circ\text{C}$  in a nitrogen atmosphere. Afterward, it was quenched with 1.5 L of ethanol and washed three times with  $800 \text{ cm}^3$  of ethanol using the previously described homogenization–centrifugation step. The modified BCN was flash frozen at a concentration of  $0.4\% \text{ (g mL}^{-1}\text{)}$  in dimethyl carbonate by immersion in liquid nitrogen and subsequently freeze-dried (Edwards Modulyo freeze-dryer, West Sussex, U.K.) prior to use. The BCNs modified with acetic, hexanoic, and dodecanoic acids were termed C<sub>2</sub>-BCN, C<sub>6</sub>-BCN, and C<sub>12</sub>-BCN, respectively.

**2.2. Preparation of w/o Emulsions Stabilized by Modified BCN.** The emulsion preparation was adapted from a protocol described by Binks et al.<sup>32</sup> for aqueous foams stabilized solely by silica particles but modified for the use of modified BCN-stabilized emulsions. First, the modified BCN was dispersed in toluene at a concentration of  $0.5\% \text{ (g mL}^{-1}\text{)}$  using a homogenizer operating at 20000 rpm for 1 min. Water was then added into the dispersion to produce a water volume fraction ( $\phi_w$ ) of either 50% or 60%, depending on the experiments conducted. This water/oil/modified BCN dispersion was shaken by hand for 10 min at 4 Hz to create the w/o particle-stabilized emulsions.

**2.3. Characterization of (Modified) BCN and the w/o emulsions.** Dynamic vapor sorption (DVS) was used to quantify the water and toluene uptake of neat and modified BCN. This measurement was carried out using a DVS Advantage (Surface Measurement Systems Ltd., Alperston, U.K.). Approximately 30 mg of freeze-dried (modified) BCN was placed in the sample chamber and

preconditioned at 0% partial pressure (in air) for 5 h to remove any adsorbed water molecules. The partial pressure of the solvent in the sample chamber was then increased to 90% for 10 h to allow for the adsorption of the solvent molecules onto (modified) BCN, and the mass change during this adsorption process was recorded in situ as a function of time. The water or toluene uptake of the (modified) BCN was evaluated by taking the ratio between the mass change of (modified) BCN due to adsorption of water or toluene at 90% partial pressure and the dry mass of (modified) BCN. The degree of surface substitution (DSS) of the modified BCN was quantified by determining the amount of surface hydroxyl groups on both neat and modified BCN using the DVS Advantage. For this, deuterium oxide was used as the solvent instead of water to exchange the hydroxyl group hydrogen atom into deuterium. Briefly, the same amount of previously mentioned freeze-dried (modified) BCN was placed in the sample chamber and preconditioned at 0% partial pressure of deuterium oxide for 5 h to remove any adsorbed water molecules. The partial pressure of deuterium oxide was then increased to 90% for 2 h and decreased to 0% for another 2 h. This adsorption–desorption cycle was repeated 10 times. Such a short adsorption cycle was used to avoid bulk sorption of deuterium oxide in BCN. The sample was then postconditioned at 0% partial pressure for another 5 h. As the deuterium atom is one neutron heavier than hydrogen, this mass increase after postconditioned BCN can be measured by the ultrasensitive microbalance, and the amount of accessible hydroxyl groups can be back-calculated from this mass gain using the following equation:

$$\Delta m = \frac{(\text{OH})m_i N_A m_n}{162140} \quad (2)$$

where  $\Delta m$  is the mass change after hydrogen–deuterium exchange (mg), OH the number of accessible hydroxyl groups,  $m_i$  the initial mass of sample (mg),  $N_A$  Avogadro's number, and  $m_n$  the mass of a neutron (mg). The number 162140 represents the molecular mass of a single glucose unit ( $\text{C}_6\text{H}_{10}\text{O}_5$ ) having units of milligrams per mole.

Inverse gas chromatography (IGC) was used to determine the nonspecific surface energy of neat and modified BCN.<sup>33–35</sup> Dorris and Gray<sup>36</sup> have suggested that the Gibbs free energy of adsorption ( $\Delta G$ ) is related to the work of adhesion ( $W_a$ ) via

$$-\Delta G = aN_A W_a \quad (3)$$

where  $a$  and  $N_A$  represent the area covered by the probe molecules and Avogadro's number, respectively. When nonpolar (*n*-alkanes) probes are used, only nonspecific interaction between the substrate and probe molecules occurs. The resulting  $W_a$  is then defined as

$$W_a = 2(\gamma_s^d \gamma_l^d)^{1/2} \quad (4)$$

where  $\gamma_s^d$  and  $\gamma_l^d$  denote the dispersive surface energies of the substrate and the probe, respectively.<sup>37</sup> Combining eqs 3 and 4 and substituting  $-\Delta G = RT \ln(V_n)$

$$RT \ln(V_n) = 2aN_A(\gamma_s^d)^{1/2}(\gamma_l^d)^{1/2} + C \quad (5)$$

Therefore,  $\gamma_s^d$  can be determined from the slope of the plot of  $RT \ln(V_n)$  against  $a(\gamma_l^d)^{1/2}$ .

To measure the  $\gamma_s^d$  of neat and modified BCN, approximately 50 mg of sample was packed into a 4 mm internal diameter glass column between silanized glass wool. The samples were held at  $30 \text{ }^\circ\text{C}$  and 0% relative humidity (RH) in He for 2 h to remove any residual moisture in the samples. A series of alkane vapors (pentane, hexane, heptane, octane, and nonane) were used as nonpolar probes for evaluating  $\gamma_s^d$  of the samples. Methane was used to determine the dead time of the packed column. The probes were injected under infinite dilution at a concentration of 3 vol %. The retention volumes of these probe molecules were determined by peak maximum analysis using an SMS-iGC 2000 instrument (Surface Measurement Systems Ltd.).  $\gamma_s^d$  of neat and modified BCN was calculated on the basis of a method proposed by Schultz et al.<sup>38</sup> The measurements were duplicated.

**Table 2. Summary of Water and Toluene Uptake ( $\Delta m$ ), Relative Water and Toluene Uptake ( $\alpha$ ), Dispersive Surface Energy ( $\gamma_s^d$ ), Degree of Surface Substitution (DSS), and Degree of Crystallinity ( $\chi_c$ ) of the Neat and Modified BCN**

sample	$\Delta m_{\text{water}}$ (wt %)	$\Delta m_{\text{toluene}}$ (wt %)	$\alpha$	$\gamma_s^d$ (mJ m <sup>-2</sup> )	DSS <sup>a</sup> (%)	$\chi_c^a$ (%)
neat BCN	16.94 ± 0.01	7.30 ± 0.01	2.32 ± 0.01	65.4 ± 1.2	0	90.2 ± 0.2
C <sub>2</sub> -BCN	6.73 ± 0.01	15.02 ± 0.01	0.45 ± 0.01	48.3 ± 0.1	98.9	83.2 ± 0.2
C <sub>6</sub> -BCN	6.14 ± 0.01	28.85 ± 0.02	0.21 ± 0.01	71.5 ± 1.0	58.5	89.7 ± 0.5
C <sub>12</sub> -BCN	7.44 ± 0.01	28.12 ± 0.03	0.26 ± 0.01	53.4 ± 0.1	51.9	85.1 ± 0.9

<sup>a</sup>From ref 28.

The stability of the w/o particle-stabilized emulsions was assessed by monitoring the settling of the w/o emulsion boundary as result of sedimentation. The movement of the emulsion boundary was monitored visually as a function of time. The emulsion stability index (ESI) was calculated by taking the ratio between the height of the emulsion at the time of assessment and the total volume of the mixture. The emulsion droplets were observed using a reflective optical microscope (Olympus BX 41 M, Essex, U.K.).

### 3. RESULTS AND DISCUSSION

**3.1. Water/Toluene Uptake of Neat and Modified BCN.** The water and toluene uptake of neat and modified BCN was measured, and the values are tabulated in Table 2. Neat BCN exhibited the highest water and the lowest toluene uptake compared to modified BCN. This is attributed to the hydrophilic nature of neat BCN, which contains a large amount of hydroxyl (–OH) groups on its surface.<sup>39</sup> A decrease in water uptake and an increase in toluene uptake was observed when BCN was hydrophobized by esterification with organic acids. This hydrophobization of BCN resulted in an increased hydrophobicity of modified BCN. This observation is consistent with a previous study by us,<sup>28</sup> which showed that the water-in-air contact angle measured on (modified) BCN sheets increased from 19 ± 3° for neat BCN to 133 ± 4° for C<sub>12</sub>-BCN.

A relative uptake ratio of water to toluene (denoted as  $\alpha$ ) was defined to describe the relative hydrophilicity/oleophilicity ratio of (modified) BCN.  $\alpha$  can be viewed loosely as an equivalent to the hydrophilic–lipophilic balance of a surfactant molecule, which describes the hydrophilic and oleophilic regions of the surfactant. An  $\alpha$  value of unity indicates that BCN has the same water and toluene uptake capacities at 90% partial pressure. An  $\alpha$  value of larger than unity implies BCN has a more hydrophilic character, while an  $\alpha$  value of smaller than unity indicates it prefers toluene, i.e., BCN is more oleophilic. It was observed that C<sub>6</sub>-BCN has the smallest  $\alpha$  value, followed by C<sub>12</sub>-BCN, C<sub>2</sub>-BCN, and neat BCN, respectively (see Table 1). The large  $\alpha$  value for neat BCN is not surprising as neat BCN is very hydrophilic in nature. However, it is surprising to see that C<sub>6</sub>-BCN is more oleophilic compared to C<sub>12</sub>-BCN, which has longer aliphatic chains attached to BC. This observation can be attributed to the degree of surface substitution of BCN by different long-chain organic acids. The degree of surface substitution of C<sub>12</sub> on BCN is 12% lower than that of C<sub>6</sub> on BCN, which is a result of lower reactivity of dodecanoic acid compared to hexanoic acid.<sup>28</sup> The larger  $\alpha$  value for C<sub>2</sub>-BCN can be attributed to the higher degree of substitution of BC nanofibrils with short acetyl moieties.

**3.2. Nonspecific (Dispersive) Surface Energy of (Modified) BCN.** The total surface energy of a system can be described by the summation of a nonspecific (dispersive) component and specific (induction, dipole, or hydrogen bonding) component of surface energies.<sup>40</sup> The dispersive

surface energy is nonspecific, as it exists irrespective of the partners brought into contact.<sup>41</sup> In this study, IGC was used to determine the dispersive fraction of surface energy,  $\gamma_s^d$ , of (modified) BCN. Although this technique does not provide any information regarding the specific component of the surface energy, IGC is still preferred over conventional contact angle measurements here to determine the  $\gamma_s^d$  of a substrate, as IGC does not suffer from drawbacks such as the approach used to calculate surface energy<sup>42</sup> and complications of wetting experiments on either individual BC nanofibers or papers made thereof (roughness and wicking/capillarity effects).<sup>43</sup>  $\gamma_s^d$  of neat BCN of 65.5 mJ m<sup>-2</sup> (see Table 2) obtained in this study is in good agreement with values reported in the literature.<sup>44,45</sup> The high  $\gamma_s^d$  of neat BCN can be attributed to its high crystallinity of approximately 90%,<sup>28</sup> determined using X-ray diffraction and evaluated using Segal's equation.<sup>46</sup> Due to the low concentration of probe molecules used (i.e., the measurements are conducted at infinite dilution), the probe molecules interact preferentially with the high-energy surface sites.<sup>47,48</sup> This leads to high retention times and hence the observed high  $\gamma_s^d$  value.

When BCN was modified with acetic acid (C<sub>2</sub>) and dodecanoic acid (C<sub>12</sub>),  $\gamma_s^d$  of the modified BCN decreased to 48.3 mJ m<sup>-2</sup> (C<sub>2</sub>-BCN) and 53.6 mJ m<sup>-2</sup> (C<sub>12</sub>-BCN) (Table 2). This decrease in  $\gamma_s^d$  can be attributed to the presence of lower energy sites/moieties such as –CH<sub>3</sub> and –CH<sub>2</sub>–. The  $\gamma_s^d$  of –CH<sub>3</sub> sites such as those present in polypropylene<sup>49</sup> was found to be 40 mJ m<sup>-2</sup>, while that of –CH<sub>2</sub>– sites such as those present in polyethylene was found to be 28 mJ m<sup>-2</sup>.<sup>50</sup> Therefore, it is postulated that the incorporation of these two moieties with lower  $\gamma_s^d$  than neat BCN will result in a decrease in the overall  $\gamma_s^d$  of modified BCN. In addition to this, the difference in  $\gamma_s^d$  between C<sub>2</sub>-BCN and C<sub>12</sub>-BCN could also be attributed to the difference in the degree of substitution between the modified BCNs. C<sub>2</sub>-BCN was found to possess a degree of surface substitution of 98.9%, while C<sub>12</sub>-BCN has a degree of surface substitution of only 51.9%, and therefore, the  $\gamma_s^d$  of C<sub>2</sub>-BCN is expected to be lower than that of C<sub>12</sub>-BCN. The lower  $\gamma_s^d$  of C<sub>2</sub>-BCN could also be ascribed to the lower crystallinity of C<sub>2</sub>-BCN (83.2%). It is interesting to note that C<sub>6</sub>-BCN possesses a  $\gamma_s^d$  of 71.5 mJ m<sup>-2</sup>, which is higher than that of neat BCN. Since the *n*-alkane probe molecules can only interact through a nonspecific component of the surface, this increase in  $\gamma_s^d$  is a direct result of the relatively high hydrophobicity of C<sub>6</sub>-BCN. This result corroborates the  $\alpha$  value of C<sub>6</sub>-BCN, where minimum water and maximum toluene uptakes were observed. In addition to this, we also postulate that this could be a direct result of surface (energy) heterogeneity.<sup>33</sup> This is the limitation of IGC, and it is outside the scope of the current study.

**3.3. Time-Dependent Behavior of w/o Emulsions Stabilized by Modified BCN.** Photographs of w/o MIPES with  $\phi_w = 50\%$  stabilized by C<sub>2</sub>, C<sub>6</sub>, and C<sub>12</sub>-modified BCN

are presented in Figure 2. When  $C_2$ -BCN was first dispersed in the water–toluene mixture by homogenization followed by

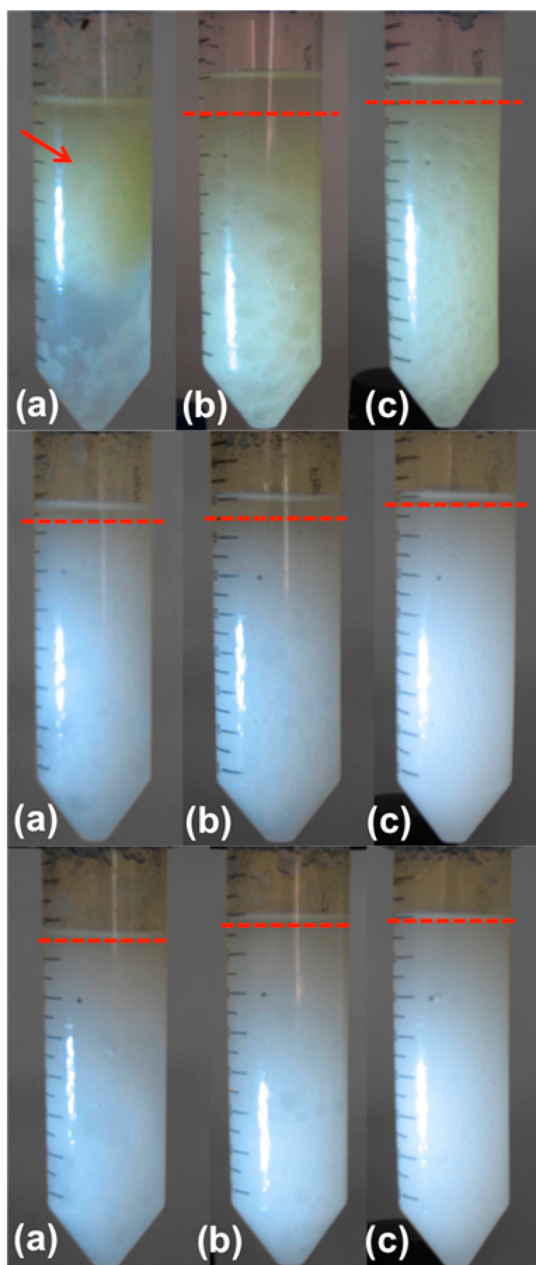


**Figure 2.** Water-in-oil emulsions stabilized by  $C_2$ -BCN (top),  $C_6$ -BCN (middle), and  $C_{12}$ -BCN (bottom) after (a) 1 day, (b) 4 days [2 days for  $C_6$ -BCN], and (c) 7 days.

hand shaking (Figure 2a, top),  $C_2$ -BCN was found to aggregate in the toluene phase (see the arrow). This tendency of  $C_2$ -BCN to aggregate in the oil phase can be attributed to the very hydrophobic nature of the modified BCN ( $\alpha < 1$ ). The  $C_2$ -BCN/toluene/water mixture was again hand shaken for 1 min at 4 Hz every 24 h, but the water phase could only be emulsified 4 days after the initial attempt of emulsification (Figure 2b, top). A homogeneous dispersion of emulsified water droplets in toluene was observed 7 days after the preparation of the emulsions (Figure 2c, top). This observation is also consistent with the hypothesis that the hydrolysis of the ester bonds is not responsible for this time-dependent behavior,

as this would result in the formation of an o/w instead of a w/o emulsion. To further verify this, we attempted to produce neat-BCN-stabilized w/o emulsions with acetic acid dissolved in the water phase. As expected, we could only produce o/w emulsions. When  $C_6$ -BCN and  $C_{12}$ -BCN were used as emulsifiers, the water phase could be emulsified instantaneously after homogenization of the water/toluene mixture with the modified BCN followed by hand shaking. However, the emulsified water phase was rather nonuniform, and very large droplets can be observed in Figure 2. Homogeneous emulsions were observed 7 days after they were initially prepared (by hand shaking for 1 min at 4 Hz every 24 h).

We hypothesize that the disentanglement and dispersion of freeze-dried modified BCN from bundles into more individualized nanofibers in toluene is responsible for the observed time-dependent behavior of these particle-stabilized emulsions (see Figure 3 for the schematic of this mechanism). In this study, the modified BCNs are expected to disperse better in the toluene phase since they are more oleophilic ( $\alpha < 1$ ). Over time, the agglomerated fiber bundles of modified BCNs loosen up until they disentangle, enabling a larger toluene–water interface to be stabilized. The formation of a stable  $C_2$ -BCN-stabilized emulsion took the longest time among the three modified-BCN-stabilized emulsions. This can be attributed to the relatively high  $\alpha$  value of  $C_2$ -BCNs compared to  $C_6$ - and  $C_{12}$ -BCNs, which implies that the disentanglement of  $C_2$ -BCNs is slower in toluene compared to that of  $C_6$ - and  $C_{12}$ -BCNs. To further verify this hypothesis, we prepared w/o emulsions using never-dried  $C_2$ -BCNs in a separate experiment. A  $C_2$ -BCN-stabilized emulsion with  $\phi_w = 50\%$  formed instantaneously upon homogenization followed by hand shaking with no observable time-dependent behavior. A homogeneous emulsion similar to those shown in Figure 2c was observed. This observation is consistent with our hypothesis, whereby time is required to disentangle the bundles/agglomerates of freeze-dried modified BCNs into individual BC nanofibers. Further confirmation of our hypothesis can also be inferred from a study conducted by Andresen et al.,<sup>18</sup> who prepared emulsions stabilized by hydrophobic microfibrillated cellulose (MFC). However, they did not observe this time dependence for their MFC-stabilized w/o emulsions, most likely because the authors never dried their MFC after modification. Their MFC was always wet, and therefore, the time-dependent behavior on the formation of homogeneous particle-stabilized emulsions was not observed.

**3.4. ESI as a Function of Time for (Modified) BCN-Stabilized Emulsions.** The ESIs of  $C_2$ -,  $C_6$ -, and  $C_{12}$ -BCN-stabilized w/o emulsions with  $\phi_w = 50\%$  are presented in Figure 4 as a function of time that passed after emulsification. It should be noted that  $C_2$ -BCN was not an effective emulsifier until the fourth day after the emulsions were initially prepared. Until the fourth day large bundles of BCN agglomerates could be observed in the oil phase, which with time loosened up and eventually allowed for emulsions to be stabilized. Therefore, Figure 4 (top) shows only the results starting from the fifth day onward. The ESI for all prepared emulsions decreased rapidly in the first 10 min after shaking to a steady-state value of approximately 80% (Figure 4). This rapid decrease is due to the gravity-induced sedimentation of the water droplets, which were approximately  $90 \mu\text{m}$  in diameter as determined by optical microscopy. The stability indices of these emulsions are not affected significantly by how long the emulsions were stored before being re-emulsified.

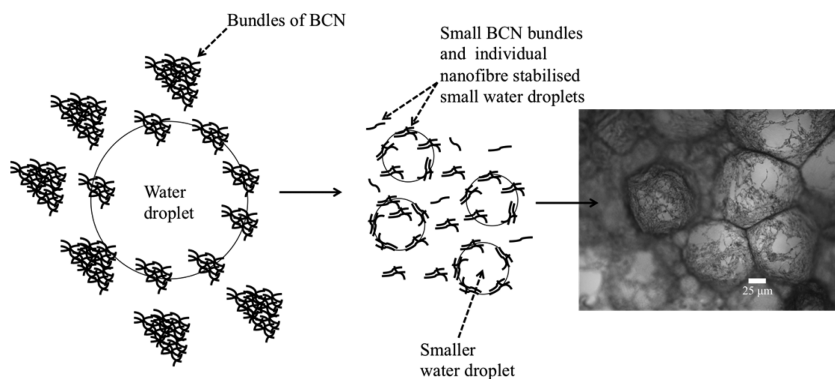


**Figure 3.** Schematic diagram showing the disentanglement of bundles of BCNs into smaller BC bundles or individualized nanofibers. Over time, the larger BCN bundles separate into smaller bundles or more individualized nanofibers in the oil phase, resulting in the stabilization of larger interfacial area. This resulted in the observed time-dependent behavior of the emulsions. The optical microscopy image shows the w/o emulsion, an HIPE, stabilized by  $C_6$ -BCNs, with bundles of  $C_6$ -BCNs adsorbing at the oil/water interface. The scale bar represents 25  $\mu\text{m}$ .

### 3.5. Catastrophic Phase Separation of the Emulsions.

An example of reversible catastrophic phase separation of particle-stabilized emulsions is shown in Figure 5. The emulsion with a  $\phi_w$  of 60% was stabilized by  $C_6$ -BCN (see Figure 5a). Sedimentation of the internal phase was observed.  $\phi_w$  was slowly increased by removing the ejected oil phase 1 mL at a time while keeping the volume of water and particle concentration relative to water constant until the particle-stabilized emulsions destabilized. After each removal step, the emulsion was hand shaken for 1 min to establish a new equilibrium. The  $C_6$ -BCN-stabilized w/o emulsion was stable until  $\phi_w = 81\%$ , transforming from an MIPE to an HIPE before catastrophic phase separation eventually occurred at  $\phi_w = 84\%$ . At this  $\phi_w$ ,  $C_6$ -BCN can be seen migrating to the oil phase due to its oleophilic character (see Figure 5b, top arrow) while the previously emulsified water phase separated to the bottom of the tube (see Figure 5b, bottom arrow). When  $\phi_w$  was decreased to 60% again by addition of fresh toluene followed by hand shaking, the emulsion re-formed (see Figure 5c). It should be noted that we did not observe catastrophic phase inversion of particle-stabilized emulsions as described by Binks et al.<sup>51</sup> They observed that an emulsion could phase invert from w/o to o/w or vice versa upon increasing the dispersed phase volume. Although the mechanism of catastrophic phase inversion in particle-stabilized emulsions is still unknown, it seems that phase inversion is not a universal phenomenon in particle-stabilized emulsions. We hypothesize that large BCN networks bridge droplets through the thin continuous films of oil phase separating droplets (see Figure 3), preventing the phase inversion of these w/o emulsions. As a result of this bridging of droplets by BCN networks adsorbed to the w/o interfaces, the BCN lacks the degree of freedom to reorientate to form an o/w emulsion. We postulate that therefore phase separation is observed when  $\phi_w$  increases.

Due to the time taken to fully disentangle the bundles of freeze-dried modified BCNs, the  $\phi_w$  at which this catastrophic phase separation occurs was also found to be a function of time (Figure 6). In addition to this,  $\phi_w$  reaches an equilibrium maximum value, which corresponds to fully disentangled BCNs stabilizing the toluene–water interface. No additional interface can be stabilized at the same BCN concentration. This catastrophic phase separation boundary of the particle-stabilized emulsion varies for the various modified BCNs, which differ with respect to their hydrophobicity.  $C_2$ -BCN was able to stabilize w/o emulsions with a maximum dispersed

phase volume ratio  $\phi_w$  of  $\sim 71\%$ , followed by  $C_{12}$ -BCN ( $\sim 77\%$ ) and  $C_6$ -BCN ( $\sim 81\%$ ). The wettability of the particle is known to affect the emulsion stability but also the maximum attainable  $\phi_w$ , as shown by Binks and Lumdsom<sup>51</sup> experimentally and later by Kaptay theoretically.<sup>52</sup> Kaptay has theoretically, with some assumptions, shown the phase inversion point in a plot of the volume fraction of the water phase as a function of the particle contact angle. Both studies demonstrated that the maximum  $\phi_w$  increases with increasing particle hydrophobicity, which is in good agreement with our findings showing that with increasing relative toluene and water uptake ( $\alpha^{-1}$  value), in the order  $C_2$ -BCN >  $C_{12}$ -BCN >  $C_6$ -BCN, i.e., with increasing hydrophobicity of the BCN, the maximum  $\phi_w$  increased.

Binks et al.<sup>51,53</sup> plotted a phase diagram relating the volume fraction at the point of catastrophic phase inversion and the wettability of the particles to the type of emulsions which could be stabilized. In this study, a similar approach was taken to quantify the boundary at which catastrophic phase separation of emulsions stabilized by modified BCN occurs. By assuming that the  $\alpha$  value is equivalent to the HLB value for the modified BCN, a phase separation boundary relating the relative hydrophilic-to-oleophilic character of the modified BCN to the types of emulsions and the maximum attainable  $\phi_w$  was plotted (see Figure 7). [Figure 7 was plotted against  $\alpha^{-1}$  instead of  $\alpha$  to denote the increase in relative hydrophobicity on the y-axis (mimicking the HLB versus  $\phi_w$  curve for surfactant-stabilized emulsions as a higher HLB value corresponds to a higher lipophilic balance).] As a result of the disentanglement and dispersion of the modified BCN, the maximum attainable  $\phi_w$  increases as a function of time, resulting in a shift of the phase boundary toward higher  $\phi_w$  until the modified BCN is dispersed into more individualized nanofibers. The region to the left of the boundary indicates the formation of stable w/o emulsions, and the region to the right of the boundary indicates fully phase-separated mixtures of water and toluene, rather than phase-inverted (low internal phase) emulsions. However, the transition between w/o emulsions and phase separation is reversible. We attribute this to the surface-active nature of the modified BCNs, which tend to prefer the oil–water interface to the oil phase because this is more thermodynamically favorable.

## 4. CONCLUSIONS

The behavior of medium and high internal phase w/o emulsions stabilized by hydrophobized BCN was studied in this work. The BCN was modified by esterification with organic

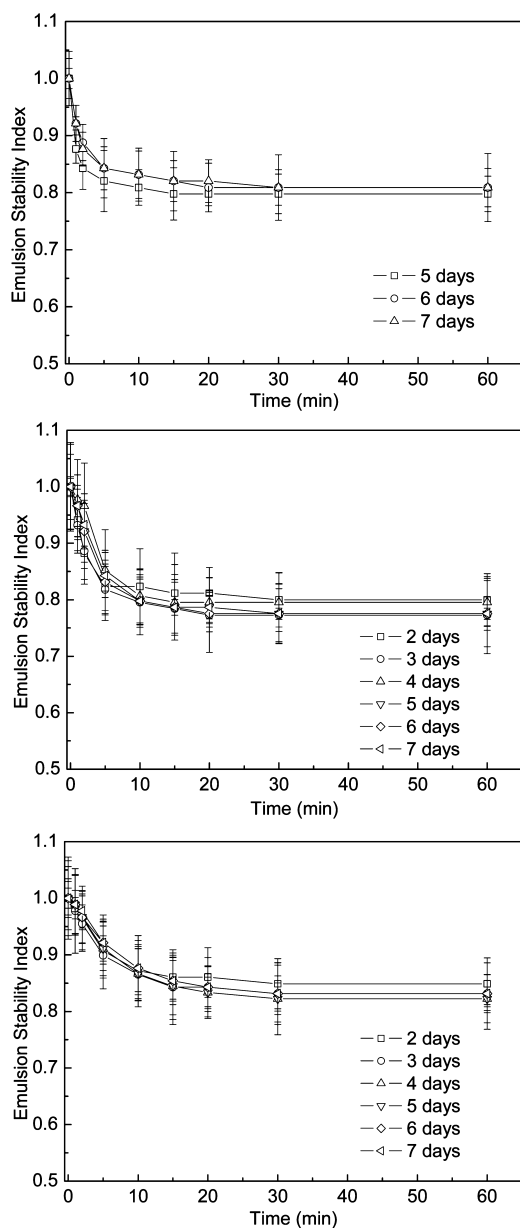


**Figure 4.** Emulsion stability indices (ESIs) of  $C_2$ -BCN-stabilized (top),  $C_6$ -BCN-stabilized (middle), and  $C_{12}$ -BCN-stabilized (bottom) emulsions as a function of time after initial emulsification. The emulsions were hand shaken every 24 h prior to monitor the decrease in height of the emulsions due to sedimentation. The number of days in the figure legend indicates the number of days after initial emulsification.

acids of different chain lengths, namely, acetic ( $C_2$ ), hexanoic ( $C_6$ ), and dodecanoic ( $C_{12}$ ) acids, to render the otherwise hydrophilic surface of BCN hydrophobic. The organic acid-modified BCN proved to be an excellent emulsifier to produce a stable concentrated w/o emulsion. The formation of the emulsions exhibited a time-dependent behavior. We attribute this to the disentanglement and dispersion of modified BCN bundles in toluene into individual nanofibers. As a result of this, the interfacial area that can be stabilized by a given concentration of modified BCN increased. In addition to this, we found that HIEPs with maximum attainable  $\phi_w$  values of 71%, 81%, and 77% for  $C_2$ -BCN-,  $C_6$ -BCN-, and  $C_{12}$ -BCN-stabilized emulsions, respectively, can be obtained. These

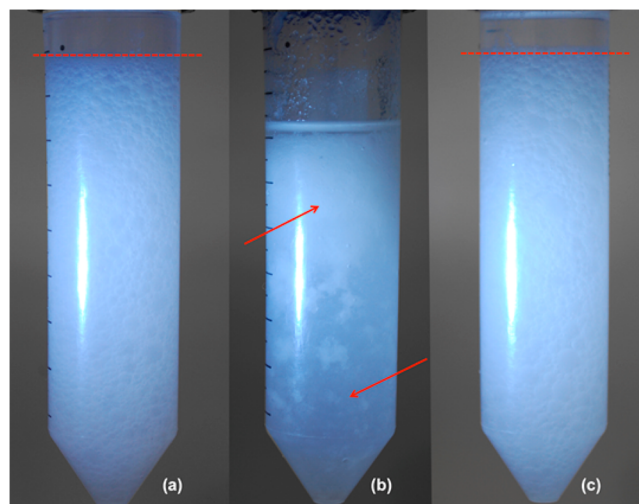


**Figure 5.** Example of reversible catastrophic phase separation for a  $C_6$ -BCN-stabilized emulsion 125 h after the emulsion was prepared. Starting with  $\phi_w = 60$  vol %, as seen in (a), the emulsion was forced to destabilize by increasing  $\phi_w$  to 84 vol %, as seen in (b). The particle-stabilized emulsion could then be re-formed by replacing the continuous phase such that  $\phi_w$  was 60 vol % again, shown in (c). The emulsions were hand shaken for 1 min at each transition. The top and bottom arrows in (b) show the  $C_6$ -BCN in the toluene phase and water phase, respectively.

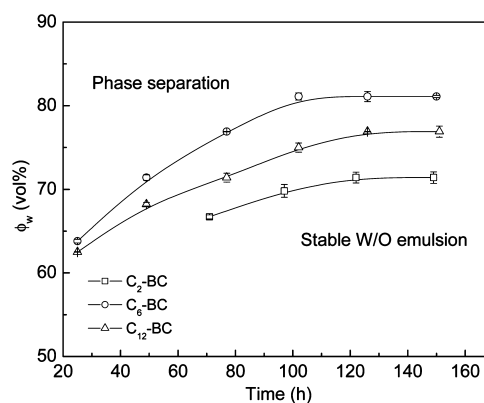


**Figure 6.** Maximum internal phase volume  $\phi_w$  as a function of time after the particle-stabilized emulsions were prepared for various modified BCNs.

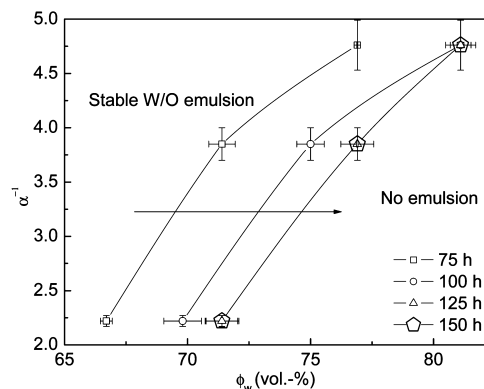


**Figure 7.** Particle-stabilized emulsion phase diagram relating the relative hydrophobicity/hydrophilicity of the BCN and the maximum achievable internal phase volume  $\phi_w$  as a function of time after the emulsions were prepared.

maximum attainable  $\phi_w$  values also exhibited a time-dependent behavior. When  $\phi_w$  increased, catastrophic phase inversion from w/o to o/w was not observed for these particle-stabilized emulsions; instead, these emulsions underwent catastrophic phase separation, which was, however, reversible. Increasing  $\phi_w$  of the w/o emulsions destabilizes the emulsions, but the w/o emulsions can be re-formed when  $\phi_w$  is reduced. This reversible phase separation boundary between w/o emulsions and phase separation is also a function of time.

## AUTHOR INFORMATION

### Corresponding Author

\*E-mail: alexander.bismarck@univie.ac.at or a.bismarck@imperial.ac.uk. Phone: +44 (0)20 7594 5578. Fax: +44 (0)20 7594 5638.

### Present Address

<sup>†</sup>Department of Chemical Engineering, University College London, Torrington Place, WC1E 7JE, London, UK.

### Notes

The authors declare no competing financial interest.

## ACKNOWLEDGMENTS

We greatly acknowledge the funding provided by the U.K. Engineering and Physical Science Research Council (EPSRC) (Grant EP/F032005/1), the University of Vienna for continuing to fund K.-Y.L., and the Challenging Engineering Programme of the EPSRC (Grant EP/E007538/1) for funding J.J.B. and R.M.

## REFERENCES

- (1) Ramsden, W. Separation of solids in the surface-layer of solution and 'suspensions' (observations on surface-membranes, bubbles, emulsions and mechanical coagulation).—Preliminary account. *Proc. R. Soc. London* **1903**, 72 (477–486), 156–164.
- (2) Pickering, S. U. Emulsions. *J. Chem. Soc., Trans.* **1907**, 91, 2001–2021.
- (3) Finkle, P.; Draper, H. D.; Hildebrand, J. H. The theory of emulsification. *J. Am. Chem. Soc.* **1923**, 45 (12), 2780–2788.
- (4) Scarlett, A. J.; Morgan, W. L.; Hildebrand, J. H. Emulsification by solid powders. *J. Phys. Chem.* **1926**, 31 (10), 1566–1571.
- (5) Koretzki, A. F.; Kruglyakov, P. M. Emulgirovaniye deistvie tvoridich chastic I energetika ich smachivaniia na granice razdela vodamaslo. *Izv. Sib. Otd. Akad. Nauk SSSR, Ser. Khim. Nauk* **1971**, 2 (1), 139–141.
- (6) Scheludko, A.; Toshev, B. V.; Bojadjev, D. T. Attachment of particles to a liquid surface (capillary theory of flotation). *J. Chem. Soc., Faraday Trans. 1* **1976**, 72, 2815–2828.
- (7) Levine, S.; Bowen, B. D.; Partridge, S. J. Stabilization of emulsions by fine particles. 1. Partitioning of particles between continuous phase and oil-water interface. *Colloids Surf.* **1989**, 38 (4), 325–343.
- (8) Binks, B. P. Particles as surfactants—Similarities and differences. *Curr. Opin. Colloid Interface Sci.* **2002**, 7 (1–2), 21–41.
- (9) Aveyard, R.; Binks, B. P.; Clint, J. H. Emulsions stabilised solely by colloidal particles. *Adv. Colloid Interface Sci.* **2003**, 100, 503–546.
- (10) Horozov, T. S.; Binks, B. P. Particle-stabilized emulsions: A bilayer or a bridging monolayer? *Angew. Chem., Int. Ed.* **2006**, 45 (5), 773–776.
- (11) Abend, S.; Bonnke, N.; Gutschner, U.; Lagaly, G. Stabilization of emulsions by heterocoagulation of clay minerals and layered double hydroxides. *Colloid Polym. Sci.* **1998**, 276 (8), 730–737.
- (12) Arditty, S.; Whitby, C. P.; Binks, B. P.; Schmitt, V.; Leal-Calderon, F. Some general features of limited coalescence in solid-stabilized emulsions. *Eur. Phys. J. E* **2003**, 11 (3), 273–281.

- (13) Fujii, S.; Read, E. S.; Binks, B. P.; Armes, S. P. Stimulus-responsive emulsifiers based on nanocomposite microgel particles. *Adv. Mater.* **2005**, 17 (8), 1014–+.

- (14) Oza, K. P.; Frank, S. G. Microcrystalline cellulose stabilized emulsions. *J. Dispersion Sci. Technol.* **1986**, 7 (5), 543–561.

- (15) Ougiya, H.; Watanabe, K.; Morinaga, Y.; Yoshinaga, F. Emulsion-stabilizing effect of bacterial cellulose. *Biosci., Biotechnol., Biochem.* **1997**, 61 (9), 1541–1545.

- (16) Zoppe, J. O.; Venditti, R. A.; Rojas, O. J. Pickering emulsions stabilized by cellulose nanocrystals grafted with thermo-responsive polymer brushes. *J. Colloid Interface Sci.* **2012**, 369, 202–209.

- (17) Lif, A.; Stenstad, P.; Syverud, K.; Nyden, M.; Holmberg, K. Fischer–Tropsch diesel emulsions stabilised by microfibrillated cellulose and nonionic surfactants. *J. Colloid Interface Sci.* **2010**, 352 (2), 585–592.

- (18) Andresen, M.; Stenius, P. Water-in-oil emulsions stabilized by hydrophobized microfibrillated cellulose. *J. Dispersion Sci. Technol.* **2007**, 28 (6), 837–844.

- (19) Khanari, K.; Syverud, K.; Stenius, P. Emulsions stabilized by microfibrillated cellulose: The effect of hydrophobization, concentration and o/w ratio. *J. Dispersion Sci. Technol.* **2011**, 32 (3), 447–452.

- (20) Kalashnikova, I.; Bizot, H.; Bertoncini, P.; Cathala, B.; Capron, I. Cellulosic nanorods of various aspect ratios for oil in water Pickering emulsions. *Soft Matter* **2013**, 9 (3), 952–959.

- (21) Kalashnikova, I.; Bizot, H.; Cathala, B.; Capron, I. New Pickering emulsions stabilized by bacterial cellulose nanocrystals. *Langmuir* **2011**, 27 (12), 7471–7479.

- (22) Kalashnikova, I.; Bizot, H.; Cathala, B.; Capron, I. Modulation of cellulose nanocrystals amphiphilic properties to stabilize oil/water interface. *Biomacromolecules* **2012**, 13 (1), 267–275.

- (23) Capron, I.; Cathala, B. Surfactant-free high internal phase emulsions stabilized by cellulose nanocrystals. *Biomacromolecules* **2013**, 14 (2), 291–296.

- (24) Blaker, J. J.; Lee, K. Y.; Li, X. X.; Menner, A.; Bismarck, A. Renewable nanocomposite polymer foams synthesized from Pickering emulsion templates. *Green Chem.* **2009**, 11 (9), 1321–1326.

- (25) Dunstan, T. S.; Fletcher, P. D. I.; Mashinchi, S. High internal phase emulsions: Catastrophic phase inversion, stability, and triggered destabilization. *Langmuir* **2012**, 28 (1), 339–349.

- (26) Cameron, N. R. High internal phase emulsion templating as a route to well-defined porous polymers. *Polymer* **2005**, 46 (5), 1439–1449.

- (27) Lee, K.-Y.; Blaker, J. J.; Bismarck, A. Surface functionalisation of bacterial cellulose as the route to produce green polylactide nanocomposites with improved properties. *Compos. Sci. Technol.* **2009**, 69 (15–16), 2724–2733.

- (28) Lee, K.-Y.; Quero, F.; Blaker, J. J.; Hill, C. A. S.; Eichhorn, S. J.; Bismarck, A. Surface only modification of bacterial cellulose nanofibres with organic acids. *Cellulose* **2011**, 18 (3), 595–605.

- (29) Toyosaki, H.; Naritomi, T.; Seto, A.; Matsuoka, M.; Tsuchida, T.; Yoshinaga, F. Screening of bacterial cellulose-producing acetobacter strains suitable for agitated culture. *Biosci., Biotechnol., Biochem.* **1995**, 59 (8), 1498–1502.

- (30) Lee, K.-Y.; Buldum, G.; Mantalaris, A.; Bismarck, A. More than meets the eye in bacterial cellulose: Biosynthesis, bioprocessing, and applications in advanced fiber composites. *Macromol. Biosci.* **2014**, DOI: 10.1002/mabi.201300298.

- (31) Lee, K. Y.; Bismarck, A. Susceptibility of never-dried and freeze-dried bacterial cellulose towards esterification with organic acid. *Cellulose* **2012**, 19 (3), 891–900.

- (32) Binks, B. P.; Horozov, T. S. Aqueous foams stabilized solely by silica nanoparticles. *Angew. Chem., Int. Ed.* **2005**, 44 (24), 3722–3725.

- (33) Charmas, B.; Lebeda, R. Effect of surface heterogeneity on adsorption on solid surfaces—Application of inverse gas chromatography in the studies of energetic heterogeneity of adsorbents. *J. Chromatogr., A* **2000**, 886 (1–2), 133–152.

- (34) Thielmann, F. Introduction into the characterisation of porous materials by inverse gas chromatography. *J. Chromatogr., A* **2004**, 1037 (1–2), 115–123.

- (35) Voelkel, A.; Strzemiescka, B.; Adamska, K.; Milczewska, K. Inverse gas chromatography as a source of physicochemical data. *J. Chromatogr., A* **2009**, *1216* (10), 1551–1566.
- (36) Dorris, G. M.; Gray, D. G. Adsorption of normal-alkanes at zero surface coverage on cellulose paper and wood fibers. *J. Colloid Interface Sci.* **1980**, *77* (2), 353–362.
- (37) Shen, W.; Parker, I. H. Surface composition and surface energetics of various eucalypt pulps. *Cellulose* **1999**, *6* (1), 41–55.
- (38) Schultz, J.; Lavielle, L.; Martin, C. The role of the interface in carbon-fiber epoxy composites. *J. Adhes.* **1987**, *23* (1), 45–60.
- (39) Blaker, J. J.; Lee, K. Y.; Mantalaris, A.; Bismarck, A. Ice-microsphere templating to produce highly porous nanocomposite PLA matrix scaffolds with pores selectively lined by bacterial cellulose nano-whiskers. *Compos. Sci. Technol.* **2010**, *70* (13), 1879–1888.
- (40) Kloubek, J. Development of methods for surface free-energy determination using contact angles of liquids on solids. *Adv. Colloid Interface Sci.* **1992**, *38*, 99–142.
- (41) Fowkes, F. M. Role of acid-base interfacial bonding in adhesion. *J. Adhes. Sci. Technol.* **1987**, *1* (1), 7–27.
- (42) Planinsek, O.; Trojak, A.; Srcic, S. The dispersive component of the surface free energy of powders assessed using inverse gas chromatography and contact angle measurements. *Int. J. Pharm.* **2001**, *221* (1–2), 211–217.
- (43) Buckton, G.; Darcy, P.; McCarthy, D. The extent of errors associated with contact angles. 3. The influence of surface-roughness effects on angles measured using a Wilhelmy plate technique for powders. *Colloids Surf., A* **1995**, *95* (1), 27–35.
- (44) Heng, J. Y. Y.; Pearse, D. F.; Thielmann, F.; Lampke, T.; Bismarck, A. Methods to determine surface energies of natural fibres: A review. *Compos. Interfaces* **2007**, *14* (7–9), 581–604.
- (45) Pommet, M.; Juntaro, J.; Heng, J. Y. Y.; Mantalaris, A.; Lee, A. F.; Wilson, K.; Kalinka, G.; Shaffer, M. S. P.; Bismarck, A. Surface modification of natural fibers using bacteria: Depositing bacterial cellulose onto natural fibers to create hierarchical fiber reinforced nanocomposites. *Biomacromolecules* **2008**, *9* (6), 1643–1651.
- (46) Segal, L.; Creely, J. J.; Martin-Jr, A. E.; Conrad, C. M. An empirical method for estimating the degree of crystallinity of native cellulose using the X-ray diffractometer. *Text. Res. J.* **1959**, *29* (10), 786–794.
- (47) Ho, R.; Heng, J. Y. Y. A review of inverse gas chromatography and its development as a tool to characterize anisotropic surface properties of pharmaceutical solids. *KONA Powder Part. J.* **2013**, No. 30, 164–180.
- (48) Jefferson, A. E.; Williams, D. R.; Heng, J. Y. Y. Computing the surface energy distributions of heterogeneous crystalline powders. *J. Adhes. Sci. Technol.* **2011**, *25* (4–5), 339–355.
- (49) Calhoun, A. A.; Nicholson, P. D.; Barnes, A. B. The use of inverse gas chromatography to study surface thermal oxidation of polypropylene. *Polym. Degrad. Stab.* **2006**, *91* (9), 1964–1971.
- (50) Jandura, P.; Riedl, B.; Kokta, B. V. Inverse gas chromatography study on partially esterified paper fiber. *J. Chromatogr., A* **2002**, *969* (1–2), 301–311.
- (51) Binks, B. P.; Lumsdon, S. O. Catastrophic phase inversion of water-in-oil emulsions stabilized by hydrophobic silica. *Langmuir* **2000**, *16* (6), 2539–2547.
- (52) Kaptay, G. On the equation of the maximum capillary pressure induced by solid particles to stabilize emulsions and foams and on the emulsion stability diagrams. *Colloids Surf., A* **2006**, *282*, 387–401.
- (53) Binks, B. P.; Lumsdon, S. O. Influence of particle wettability on the type and stability of surfactant-free emulsions. *Langmuir* **2000**, *16* (23), 8622–8631.
- (54) Oza, K. P.; Frank, S. G. Multiple emulsions stabilized by colloidal microcrystalline cellulose. *J. Dispersion Sci. Technol.* **1989**, *10* (2), 163–185.
- (55) Oza, K. P.; Frank, S. G. Drug release from emulsions stabilized by colloidal microcrystalline cellulose. *J. Dispersion Sci. Technol.* **1989**, *10* (2), 187–210.
- (56) Kargar, M.; Fayazmanesh, K.; Alavi, M.; Spyropoulos, F.; Norton, I. T. Investigation into the potential ability of Pickering emulsions (food-grade particles) to enhance the oxidative stability of oil-in-water emulsions. *J. Colloid Interface Sci.* **2012**, *366* (1), 209–215.